

# Probing optical microfiber nonuniformities at nanoscale

M. Sumetsky, Y. Dulashko, J. M. Fini, A. Hale, and J. W. Nicholson

*OFS Laboratories, 19 Schoolhouse Road, Somerset, New Jersey 08873*

Received May 2, 2006; revised May 24, 2006; accepted June 2, 2006;  
posted June 8, 2006 (Doc. ID 70530); published July 25, 2006

We demonstrate a novel, simple, and comprehensive method for probing optical microfiber surface and bulk distortions with subnanometer accuracy. The method employs a regular optical fiber as a probe that slides along a microfiber transmitting the fundamental mode. The fraction of radiation power absorbed in the probe depends on the local distribution of the mode propagating in the microfiber. From the measured variation of the absorbed power, we determine the variation of the effective microfiber radius, which takes into account both the microfiber radius and refractive index variations. Furthermore, we verify the cylindrical symmetry of the microfiber nonuniformities by probing the microfiber from different sides. These results explain observed transmission losses in silica microfibers and open broad opportunities for microfiber investigation. © 2006 Optical Society of America  
*OCIS codes:* 060.2340, 060.2370.

Optical microfibers (MFs) have recently been proposed as building blocks for micro-optical devices with applications in photonics, physics, chemistry, and biology.<sup>1–6</sup> Important advantages of MFs are the potential for compact 3D assembly, the possibility of strong coupling to the environment and/or localization of radiation, and low transmission loss. To date, the lowest experimentally achieved loss of a single-mode MF is  $\sim 0.01$  dB/cm (Ref. 3), and this can be further reduced with advances in the MF drawing technique.

The dominant contribution to MF loss is due to both surface and bulk nonuniformities such as surface contamination, corrosion, frozen-in microdeformations,<sup>7</sup> and microstresses. According to theoretical estimates, to evaluate ultralow transmission losses, the corresponding transverse distortion of the MF refractive index should be characterized at the nanometer level.<sup>7,8</sup> However, to our knowledge, experimental methods capable of detecting surface and bulk nonuniformities of MF with this accuracy have not been developed. In fact, scanning electron microscopy<sup>1–3</sup> (SEM) and atomic force microscopy measurements of only the surface nonuniformity are insufficient to characterize the total MF loss. On the other hand, application of transmission electron microscopy, scanning near-field optical microscopy, and other side-scattering methods are problematic due to alignment and focusing difficulties caused by small transversal geometry and vibration of the MF. For this reason, determination of the optical MF nonuniformities at nanoscale and their effect on the MF transmission loss have remained unsolved.

In this Letter, we present a simple measurement tool to probe the electromagnetic mode propagating along the MF, and consequently, perform the comprehensive characterization of the MF nonuniformities. We experimentally determine the effective MF radius variation (combining the effects of MF surface and index variations) and achieve subnanometer accuracy with remarkable reproducibility. Analysis of our ex-

perimental data explains the observed MF propagation losses.

Our measurement setup, illustrated in Fig. 1, consists of a partly stripped 125  $\mu\text{m}$  diameter fiber segment used as a probe, and a fiber taper fabricated from SMF-28 with a uniform waist of  $\sim 4$  mm length and  $\sim 0.53$   $\mu\text{m}$  radius. The total length of the fiber taper is 36 mm, and its total loss is 0.25 dB. The taper is drawn with the CO<sub>2</sub> laser technique.<sup>5</sup> Light is launched into the taper at one end and is detected by an optical spectrum analyzer (OSA) at the other end. At the measurement wavelength (1530 nm), the taper's waist is a single-mode MF. The MF is positioned in direct contact with the fiber probe and normal to its axis. The probe is translated along the MF and, simultaneously, the transmission power is detected by an OSA. To reduce the measurement noise, the OSA is set to average multiple data points, so that we take more than 100 measurements per 1  $\mu\text{m}$  of the MF length. The MF can be tested from different sides by rotation of the MF with respect to the probe as illustrated in Fig. 1.

A fraction of the propagating light is scattered into the probe fiber and absorbed by its coating, while the remaining part is subject to the MF losses and then is detected by an OSA. The power absorbed by the

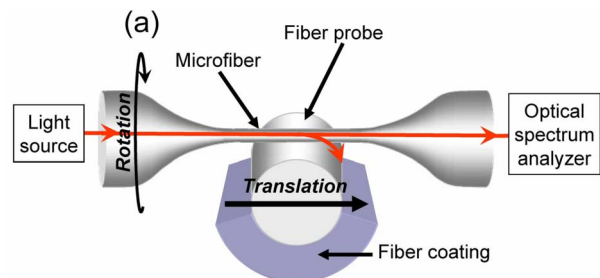


Fig. 1. (Color online) Illustration of the measurement method. A partly stripped fiber probe slides along the MF. Different sides of the MF can be tested by rotation of the MF with respect to the probe.

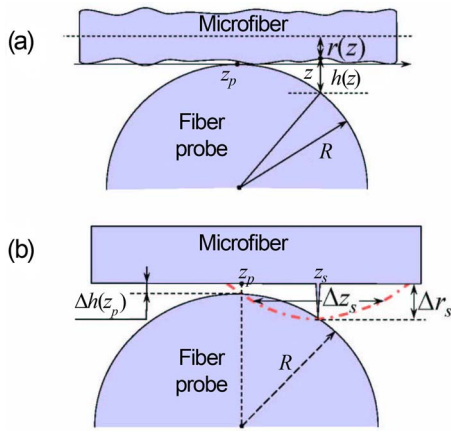


Fig. 2. (Color online) (a) Cross-sectional geometry of the MF-probe contact; (b) model of a spike at the MF surface. Dotted-dashed curve is the trajectory of the probe.

probe positioned at point  $z_p$  [see Fig. 2(a)] can be expressed through the local MF attenuation constant  $\alpha_p(z, z_p)$ :

$$T = \exp \left[ -2 \int_{-\infty}^{+\infty} \alpha_p(z, z_p) dz \right]. \quad (1)$$

Assume, first, that the characteristic length of MF nonuniformities is large enough. Then, from a simple dimensional analysis, the propagation constant depends on the radiation wavelength,  $\lambda$ , the MF radius,  $r$ , and the local gap between the probe and the MF,  $h$ , in the form  $\alpha_p = g(r/\lambda, h/\lambda)/r$ , where  $g$  is a dimensionless function. For a locally uniform MF, we find from Fig. 2(a) that  $h = (z - z_p)^2 / (2R)$ . Then Eq. (1) can be transformed to

$$T = \exp \left[ -\sqrt{R\lambda} f(r/\lambda)/r \right]. \quad (2)$$

Here  $f(x)$  is a function that is universal for our problem. This function is found by calculating the propagation constant numerically using the 2D finite-difference method, applying it to cross sections normal to the light propagation direction corresponding to different  $h$ . In the region of our interest, for  $\lambda/r$  varying in the interval between 2 and 3.6, we have found that, with excellent accuracy,  $f(x)$  is a linear function of  $x$ . For the light that is  $p$  polarized at the axis of symmetry in Fig. 2(a) (uniform MF),  $f(x) = -0.124 + 0.098x$ , while for the  $s$ -polarized light this function is only less than 2% different. From the latter equation and Eq. (2), the change in transmission loss in decibels,  $10\Delta \log[T(z)]$ , as a function of the probe position  $z$ , can be expressed through the relatively small change in the MF radius,  $\Delta r(z)$ , as

$$10\Delta \log[T(z)] = C\Delta r(z), \quad (3)$$

$$C = \sqrt{\lambda R} (0.54r - 0.85\lambda)/r^3. \quad (4)$$

Assuming, e.g.,  $r = 0.5 \mu\text{m}$ ,  $\lambda = 1.5 \mu\text{m}$ , and  $R = 62.5 \mu\text{m}$ , we estimate the constant  $C$  from Eq. (3) as  $C \approx 78 \text{ dB}/\mu\text{m}$ . Equations (3) and (4) are formally valid if the relative change of  $\Delta r(z)$  is small along the integration length of Eq. (1). For the parameters of

our problem, this length is  $\sim 7 \mu\text{m}$ . However, the spatial resolution of our method can be much smaller than this length. In fact, in the approximation considered, the attenuation constant depends on the coordinate  $z$  and position of the probe  $z_p$  only through the local microfiber radius variation,  $\Delta r(z)$ , and the distance to the probe fiber,  $h(z, z_p)$  [see Fig. 2(a)]. Because  $\Delta r(z)$  and  $h(z_p, z_p)$  are relatively small, we can write

$$\alpha_p[\Delta r(z), h(z, z_p)] = \alpha_p[0, (z - z_p)^2 / 2R] + \left( \frac{\partial \alpha_p}{\partial \Delta r} - \frac{\partial \alpha_p}{\partial h} \right) \Delta r(z) + \frac{\partial \alpha_p}{\partial h} [\Delta r(z_p) + h(z_p, z_p)], \quad (5)$$

where derivatives are taken at  $\Delta r = 0$  and  $h = (z - z_p)^2 / (2R)$ . Significantly, while  $\Delta r(z)$  is smoothed by integration in Eq. (1), the sum  $\Delta r(z_p) + h(z_p)$  is not smoothed and enables the high-resolution measurement of  $\Delta r(z)$ . Let us estimate the resolution with a model of a small width spike of the MF radius of height  $\Delta r_s$  located at  $z = z_s$ , illustrated in Fig. 2(b). For this model,  $h(z_p, z_p) = \Delta r_s - (z_p - z_s)^2 / 2R$ . The latter equation determines the FWHM of the corresponding peak in transmission as

$$\Delta z_s = 2\sqrt{\Delta r_s R}, \quad (6)$$

For example, a radius spike of 10 nm height and a width much smaller than  $1 \mu\text{m}$  will be resolved in transmission amplitude as a peak having FWHM  $\Delta z_s \sim 1.6 \mu\text{m}$ .

It follows from Eqs. (1) and (6) that, for a constant MF refractive index, the MF radius variation  $\Delta r(z)$  can be determined from  $T(z)$  by the solution of an integral equation. However, if  $\Delta r(z)$  does not significantly vary at a few micrometer scale, the approximation of Eq. (3) can be used. We consider Eq. (3) as a definition of the effective radius variation  $\Delta r(z)$ . Generally,  $\Delta r(z)$  determined from Eq. (3) includes contributions due to the MF radius variation as well as refractive index variations and can be used for further modeling and analysis of the MF nonuniformities.

Experimentally, we determine the constant  $C$  in Eq. (3) by comparison of the MF radius variation measured using SEM with the transmission power variation along the MF regions where it starts tapering. Figure 3 demonstrates good correspondence between the transmission power and SEM measurements. Along the tapered regions, the MF radius variation is large enough to be determined by SEM and the effect of index variation is relatively small. The obtained value of  $C = 88 \text{ dB}/\mu\text{m}$  (which is in reasonable agreement with the value predicted by our theory) is used to rescale the observed transmission loss variation into the effective radius variation along the MF region.

Curves 1 and 2 in Fig. 4(a) show the reproducibility of the effective radius variations measured along the  $500 \mu\text{m}$  MF segment situated near the center of the MF. Figure 4(b) shows an enlarged comparison of these curves along a  $100 \mu\text{m}$  length. The rms differ-

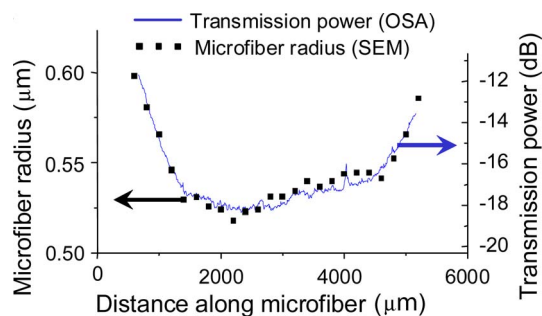


Fig. 3. (Color online) Comparison of the transmission power as a function of probe position measured by an OSA calibrated for the free MF with the MF radius variation measured by a SEM.

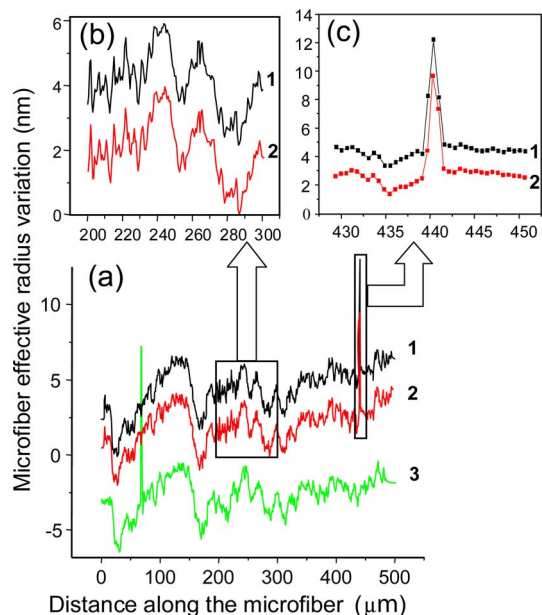


Fig. 4. (Color online) MF radius variation along a 500  $\mu\text{m}$  segment. (a) Curves 1 and 2, two measurements of this segment shifted with respect to each other along the  $y$  axis for visibility; curve 3, measurement of the same segment after MF rotation by  $90^\circ$ ; (b) curves 1 and 2 enlarged along the 100  $\mu\text{m}$  segment; (c) enlarged peaks of Fig. 4(a).

ence between curves 1 and 2 in Fig. 4(a) is 0.37 nm, while for their parts shown in Fig. 3(b) it is only 0.19 nm. Curve 3 in Fig. 4(a) is the scan of the same MF segment rotated by  $90^\circ$ . The similarity of curves 1 and 2 to curve 3 provides evidence for the axial symmetry of observed microdeformations. These curves also show two pronounced asymmetrically localized defects (sharp peaks) enlarged in Fig. 4(c). Each of them has a FWHM of  $\sim 1.5 \mu\text{m}$ . We suggest that these defects have a submicrometer width. Then their resolved FWHM is in reasonable agreement with the prediction of Eq. (6). The independence of our results to the relative initial positions of the translation stage and fiber probe, to the contact point at the probe, to small MF misalignment, to multiple repetition and reversal of scan, and to reversal of light propagation direction has been verified.

The MF attenuation constant,  $\alpha_{\text{MF}} \sim 0.05 \text{ dB/cm}$ , is estimated experimentally as the value equal to the reduction of transmission power during MF drawing

when the MF radius is reduced from 10 to  $0.53 \mu\text{m}$ . We estimate the transmission loss of the MF analytically using perturbation theory (see, e.g., Ref. 8), and find for the attenuation constant,

$$\alpha_{\text{MF}} \sim (\gamma \langle \Delta r \rangle / r)^2 \beta^{-1} \exp(-\gamma^2 L / \beta), \quad (7)$$

within a factor of the order of unity. Here  $\beta$  and  $\gamma$  are the longitudinal and transverse propagation constants of the MF, respectively,  $r$  is the MF radius,  $\langle \Delta r \rangle$  is the rms of the MF radius variation, and  $L$  is the characteristic variation length. For a regular single-mode fiber, assuming  $\langle \Delta r \rangle / r \sim 10^{-3}$ ,  $\gamma \sim 0.1 \mu\text{m}^{-1}$ ,  $\beta \sim 5 \mu\text{m}^{-1}$ , and  $L \sim 10 \mu\text{m}$ , we find  $\alpha \sim 1 \text{ dB/km}$  in reasonable agreement with numerical calculations.<sup>8</sup> For the MF under test,  $\gamma \sim 1.5 \mu\text{m}^{-1}$  and  $\beta \sim 5 \mu\text{m}^{-1}$ . From Eq. (7), the largest contribution to  $\alpha$  is made by the nonuniformities in Fig. 4 having  $\langle \Delta r \rangle / r \sim 10^{-2}$  and the smallest variation length  $L \sim 5 \mu\text{m}$ . As the result, we obtain  $\alpha \sim 0.01 \text{ dB/cm}$  in reasonable agreement with our experimental data. The loss of our MF is at least an order of magnitude greater than the estimate of the smallest possible loss, which is introduced by the frozen-in microdeformations.<sup>7</sup> This difference is, presumably, due to imperfection of our fabrication method, e.g., acceleration of translation stages and vibration of the MF during drawing.

In summary, the demonstrated experimental technique opens broad opportunities for the investigation of the MF nanoscale optical and physical properties, to improve MF quality, and broaden prospective applications of MFs in photonics and other natural sciences. The technique can be applied to the investigation of microfibers with different radii and complex internal structures (e.g., photonic crystal microfibers) by varying the radiation wavelength and considering higher-order modes. Further theoretical and experimental development of this method will allow characterization of the detailed structure of MF nonuniformities.

M. Sumetsky's e-mail address is sumetski@ofsoptics.com.

## References

1. L. Tong, R. R. Gattass, J. B. Ashcom, S. He, J. Lou, M. Shen, I. Maxwell, and E. Mazur, *Nature* **426**, 816 (2003).
2. G. Brambilla, V. Finazzi, and D. J. Richardson, *Opt. Express* **12**, 2258 (2004).
3. S. G. Leon-Saval, T. A. Birks, W. J. Wadsworth, P. St. J. Russell, and M. W. Mason, *Opt. Express* **12**, 2864 (2004).
4. H. C. Nguyen, B. T. Kuhlmeier, E. C. Mägi, M. J. Steel, P. Domachuk, C. L. Smith, and B. J. Eggleton, *Appl. Phys. B* **81**, 377 (2005).
5. M. Sumetsky, Y. Dulashko, J. M. Fini, A. Hale, and D. J. DiGiovanni, *J. Lightwave Technol.* **24**, 242 (2006).
6. M. Sumetsky, *Opt. Lett.* **31**, 87 (2006).
7. P. J. Roberts, F. Couny, H. Sabert, B. J. Mangan, T. A. Birks, J. C. Knight, and P. St. J. Russell, *Opt. Express* **13**, 7779 (2005).
8. D. Marcuse, *Appl. Opt.* **23**, 1082 (1984).